PERGAMON

Journal of Structural Geology 25 (2003) 1773–1778

JOURNAL OF STRUCTURAL GEOLOGY

www.elsevier.com/locate/jsg

Strain determinations using inoceramid shells as strain markers: a comparison of the calcite strain gauge technique and the Fry method

José M. González-Casado[a,*], Álvaro Jiménez-Berrocoso[b], Carmen García-Cuevas[a], Javier Elorza[b]

[a]*Departamento de Q.A. Geología y Geoquímica, Facultad de Ciencias, Universidad Autónoma de Madrid, 28049 Madrid, Spain*
[b]*Departamento de Mineralogía y Petrología, Universidad del País Vasco, 48080 Bilbao, Spain*

Received 25 January 2003; accepted 30 January 2003

Abstract

To test the accuracy and reliability of the strain gauge technique for calcite e-twin analysis, calcite e-twin strain and finite strain were determined using a new tectonic marker, inoceramid shells (macrofossils composed of aggregates of pseudo-hexagonal calcite prisms with a honeycomb microstructure). Although the calcite prisms in the inoceramid shells were not randomly distributed and showed strong crystallographical orientation, the strain gauge technique yields principal strain orientations that correlate precisely with those found by the Fry method. Thus, this technique can also be used to establish the ellipsoid strain orientation in rocks where calcite grains show strong crystallographical orientation.

Keywords: Strain analysis; Calcite e-twins; Strain gauge technique; Inoceramid shell

1. Introduction

The calcite strain gauge technique was developed by Groshong (Groshong, 1972, 1974; Groshong et al., 1984a) and has been successfully used to determine the finite strain in limestones moderately deformed in tectonic shallow-levels (Groshong et al., 1984a; Wiltschko et al., 1985; Craddock and Van der Pluijm, 1988; Kilsdonk and Wiltschko, 1988; Mosar, 1989; Evans and Dunne, 1991; Ferrill, 1991; Ferrill and Groshong, 1993a,b; Hindle, 1997; Harris and Van der Pluijm, 1998; González-Casado and García-Cuevas, 1999, 2002; Craddock et al., 2000). This method is based on the use of twinned calcite grains with different crystallographical orientations, scattered throughout carbonate rock, as small strain gauges. Most of the twinned grains used are in the form of coarse sparry cements or sparitic replacements. Thus, by measuring characteristics of the twinned grains, e.g. twin orientations, average twin thickness and twin density, in a small number of sparitic grains (Evans and Groshong (1994) recommended about 50 be studied), a complete strain tensor can be calculated for each sample analyzed. However, this method is limited to very small strains (0 to 11–15%; Groshong et al., 1984b), corresponding to coaxial conditions (Burkhard, 1993).

The question is whether twin strain determinations can correctly determine the bulk strain of aggregates. Comparisons between strain determinations made by the strain gauge technique and other methods of strain analysis (e.g. centre to centre, R_f/ϕ, stretched objects, etc.) are rather scarce (Burkhard, 1993), mainly due to the difficulty in using classical strain analysis methods in fine-grained limestones. To use them, appropriate strain markers (e.g. initially circular or elliptical ooids, or stretched or deformed fossils with original bilateral symmetry) and a suitable number of twinned sparry grains must be available in the same sample. Unfortunately, these conditions are rather uncommon, so comparisons have not always been adequate. Moreover, it is likely that the strain of the tectonic markers (fossils, ooids, etc.) is higher than that of the microcrystalline matrix, because of their different mechanical competence (stress risers of Ramsay and Huber (1983)) and strain partitioning.

The uncertainties related to strain partitioning can be minimized by establishing the average rock strain (bulk strain). This is determined using the centre to centre method

* Corresponding author. Tel.: +34-91397384; fax: +34-913974900.
E-mail address: g.casado@uam.es (J.M. González-Casado).

0191-8141/03/$ - see front matter © 2003 Elsevier Ltd. All rights reserved.
doi:10.1016/S0191-8141(03)00040-3

of Fry (1979), which allows the finite strain to be determined under certain conditions (Ramsay and Huber, 1983). It also allows the fabric shape of the strain markers to be assessed. However, to use this method, an aggregate of particles (calcite grains), statistically uniform in size, must have existed before deformation took place—an extremely infrequent condition in many limestones. The characteristics of the samples used in the present study allowed both methods to be used (centre to centre and strain gauge), and therefore allowed comparisons to be made between them. A widespread marine bivalve macrofossil, the inoceramid shell (Fig. 1a and b), which consists almost entirely of a lattice of sparry pseudo-hexagonal calcite prisms with a honeycomb microstructure (Fig. 1c), was used as a strain marker. On most occasions, when the bulk rock was deformed, the inoceramid shell microstructure was abundantly twinned (Fig. 1c), allowing the bulk strain to be rapidly determined using the Fry method, as well as permitting the accurate calculation of the strain related to calcite e-twinning. The purpose of this study was therefore to investigate the precision and accuracy of the calcite strain gauge technique using inoceramid shells as strain markers, comparing the results with those obtained by the Fry method. An additional aim was to evaluate the strain partitioning between e-twin and other mechanisms, such as grain boundary sliding, grain rotation and pressure solution.

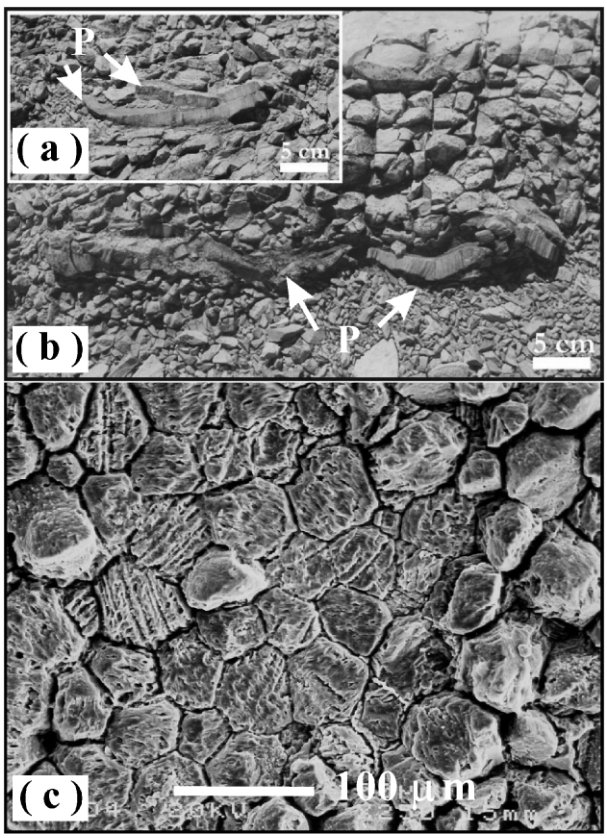

Fig. 1. (a) and (b) Two specimens of bivalve inoceramid shells from the Barrika cliff area (upper part of the Plentzia Formation). Both show fractured valves. The coarse, prismatic layer is easily seen. P = prismatic layer. Scale bars 5 cm. (c) SEM view of the outer prismatic layer of an inoceramid shell. Note the extraordinary pseudo-hexagonal sparry calcite prism arrangement (honeycomb microstructure). Twinned grains (type I twins) are found randomly distributed throughout the sample. Scale bar 100 µm.

2. Geological setting

The studied inoceramid shells were collected in the upper part of the Plentzia Formation (Mathey, 1982), which crops out on the northeastern limb of the Biscay Synclinorium, a structure trending NW–SE within the Basque–Cantabrian Basin (Fig. 2). The Plentzia Formation is a carbonate complex (calcareous flysch) that has been interpreted as reflecting deposition in the middle-outer part of a submarine fan. It is comprised of three main units, with the inoceramid shells located in the uppermost one (Barrika cliff area) (Elorza and García-Garmilla, 1996). This unit has recently been dated as early to late Santonian (Jiménez-Berrocoso et al., 2001). The Plentzia Formation was deformed during the post-Luteciense (middle Eocene) compressive phase of the Pyrenean deformations, under low temperature conditions. Large numbers of chevron folds with vergence towards the NE, faults and small shear zones are present in the Barrika cliffs (Cuevas et al., 1982).

Inoceramids are a group of extinct pterioid bivalves that were widely distributed in Mesozoic seas. They reached their worldwide maximum diversification in the Cretaceous and eventually disappeared (at least in the Basque–Cantabrian Basin domain) 2.6 Ma before the Cretaceous–Tertiary boundary (MacLeod, 1994; MacLeod et al., 2000). Inoceramid species are believed to have inhabited a great variety of paleoenvironments, practically from the subtidal region (<100 m) to deep oceanic floors (>3000 m) (Saltzman and Barron, 1982). In the study area (Barrika cliffs), the inoceramid species *Platyceramus rhomboides*

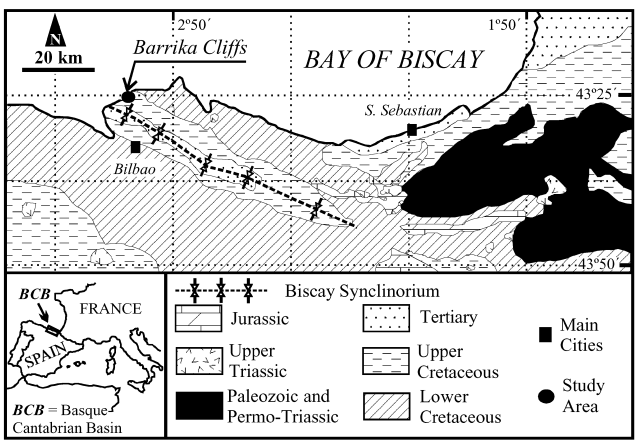

Fig. 2. Simplified geological sketch of the Biscay Synclinorium within the Basque–Cantabrian Basin. Inoceramid shells were collected in the upper part of the Plentzia Formation (Barrika cliff area) in the northeastern limb of the Synclinorium.

rhomboides (SEITZ) was the only one identified. This species is very common in early Santonian rocks of northern Spain (López et al., 1992).

Inoceramids can be either equivalves or inequivalves. Size is extremely variable, ranging from only a few centimetres to nearly two metres (some individuals from the study area were more than 80 cm long). The microstructure of the shells examined was formed of two layers: (a) a coarse prismatic outer layer, with low magnesium calcite (LMC) prisms, and (b) a thin inner layer, with an aragonitic nacreous sheet microstructure. The shells of the Barrika cliffs have only their prismatic outer layer preserved (Fig. 1a and b). The microstructure of this layer consists of parallel, simple prismatic units that do not interfinger along their boundaries, and whose longest axes are almost perpendicular to the dorsal and ventral surfaces of the shell. The prisms show a remarkable change in size between the outer and inner layers. The smaller size of the prisms in the outer layer led to its greater prismatic density than the inner layer of the shell. In thin section, perpendicular to the longest prismatic axes, the shells displayed a well-preserved polygonal honeycomb microstructure (Fig. 1c).

3. Methods

Ten samples of inoceramid shells were examined (in 2D) to compare the strain ellipsoid calculated from the calcite twins and the bulk strain established by the centre to centre method. Thin sections were made parallel to the inoceramid shell surfaces, i.e. orthogonal to the calcite prisms. For calcite twin analysis, more than 30 grains were examined in each thin section. For each grain, the e-twin orientations, *c*-axis orientation, number of twins, average thickness of twins and grain width were determined, as described by Evans and Groshong (1994), using a petrographic microscope with a U-stage. The strain ellipse orientation and ellipticity were calculated using the strain gauge technique developed by Groshong (see Groshong (1972, 1974) for a detailed description).

The bulk strain of each thin section was calculated using the centre to centre method, with more than 300 grains per thin section taken into account. In a second stage, the principal strain axis orientations and the ellipticity (R) of the strain ellipses yielded by both methods were compared in order to test the accuracy of the strain gauge technique and the strain partitioning value.

4. Results and discussion

The shape of the calcite grains in the inoceramid shells studied varied from pseudo-hexagonal to rombohedral, were generally prismatic, and varied in size from 50 to 250 μm (Fig. 1c). Generally, the calcite *c*-axes were oriented obliquely to the prisms and their distribution usually gave a strong fabric with two subhorizontal maxima always orthogonally orientated to the calcite prism (Fig. 3a). Almost all calcite grains were intensely twinned; a small fraction showed two sets of twins. In addition, the twinned grains were randomly distributed throughout the shells (Fig. 1c). The twin lamellae were thin and straight-sided, and usually extended across the entire grain. They can therefore be classified as type I twins (cf. Weiss, 1954; Ferrill, 1991; Burkhard, 1993), suggesting they underwent deformation at low temperatures and very low strain. Some samples showed incipient grain boundary sliding and sporadic detached grains along the direction of the maximum longitudinal strain. In these samples, very small calcite sparry cements were crystallized in the extension fissures. A few curved twins caused by grain deformation were also observed.

The strain gauge results provided by the calcite e-twins (Table 1) and the bulk strain values determined by the Fry method are shown in Figs. 4 and 5. The strain gauge technique allows the calculation of the lengths of the major ($1 + e_{max}$) and minor ($1 + e_{min}$) semi-axes of the finite strain ellipse, as well as their orientations and the ellipticity ($R = 1 + e_{max}/1 + e_{min}$) (Fig. 4). The obtained ellipticity values were in the range 1.01–1.03. This range is smaller than that yielded by the Fry method with the same samples

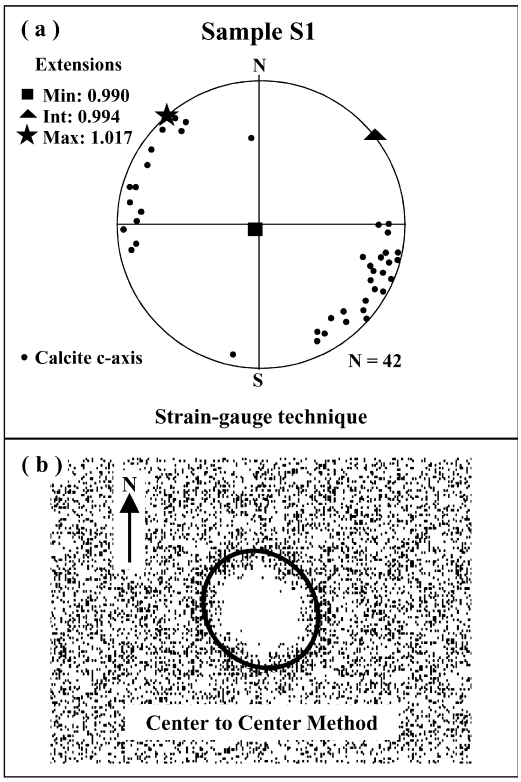

Fig. 3. Bulk strain compared with twin strain for sample S1, in a section normal to the calcite prism. (a) Results of calcite twinning analysis (strain-gauge technique). Stereographic plot of the positions of the principal strain axes. Results are given as percentages. Points represent calcite *c*-axis orientations. *N* is the number of measured grains. (b) Results of the centre to centre method.

Table 1
Results of the calcite e-twin analysis (Groshong's strain gauge technique). *N* is the number of measured grains in each sample. $(J2)^{1/2}$ is the square root of the second invariant of the strain tensor (percentage strain). NEV = negative expected values. $R = 1 + e_{max}/1 + e_{min}$. Twin density = twins/mm

Sample and (*N*)	Principal strains (bearing, value)		$(J2)^{1/2}$	Standard 'error'	NEV (%)	*R*	Density
	$1 + e_{max}$	$1 + e_{min}$					
S1 (42)	321 (1.016)	051 (0.993)	1.453	0.374	2.3	1.023	88.86
S2 (50)	163 (1.012)	259 (0.986)	1.219	0.564	4.0	1.026	85.50
S3 (50)	055 (1.014)	323 (0.989)	1.660	0.418	2.0	1.025	88.81
S4 (28)	127 (1.016)	037 (0.988)	1.459	0.796	0	1.028	125.29
S5 (30)	180 (1.011)	087 (0.998)	1.026	0.409	3.3	1.013	54.19
S6 (30)	236 (1.021)	326 (1.000)	2.131	0.975	0	1.021	108.13
S7 (49)	130 (0.982)	220 (0.966)	4.521	1.673	8.1	1.016	84.16
S8 (45)	240 (0.991)	150 (0.963)	4.208	1.015	13.3	1.029	144.78
S9 (30)	135 (1.031)	045 (1.006)	3.461	0.629	6.6	1.024	128.62
S10 (51)	021 (0.986)	112 (0.959)	4.978	1,713	9.8	1.028	127.45

(1.09–1.25). This indicates that twinning accounts for only a part of the bulk strain and that other deformation mechanisms must therefore exist. As seen in thin section, dissolution and minor recrystallization mechanisms in the prismatic honeycomb microstructure help to account for the deformation. The orientations of the dissolution planes and the small microveins (detached planes filled with calcite) correlate with the principal strain orientations found by both strain analysis methods. Thus, even under these conditions of very low deformation ($R = 1.15$), the twinning deformation mechanism alone cannot account for the strains recorded. Moreover, if the finite strain and twin strain values for each sample are compared, the increments in the bulk strain do not satisfactorily correlate with those of the twin strain (Fig. 4). This could have its origin in the small bias introduced by the e-twin analysis being performed only in thin sections normal to the calcite prism (i.e. in 2D).

In contrast, twin strain analysis revealed principal strain axis directions very similar to those obtained by the Fry method (Fig. 5). The divergence between the major semi-axis orientations calculated by the two methods varies from 3 to 31° (average 5.8°) for the $1 + e_{max}$ axis and from 3 to 30° (average 6.2°) for the $1 + e_{min}$ axis. Therefore, the twinning strain axes measured in the inoceramid shell prisms obviously record the directions of the bulk strain quite accurately. These results also suggest that twinning is contemporaneous with the other deformational mechanisms (grain boundary sliding and pressure solution) in these samples, and that all these deformational mechanisms are related to the same deformation event.

Consequently, in the analyzed samples, the strain gauge technique yields strain values that do not accurately follow the variations of the bulk strain. The twin strain results must therefore be analyzed carefully before they can be used to compare relative strain magnitudes in geological settings.

The few relationships between twin strain and finite strain that have been reported (e.g. Pfiffner and Burkhard, 1987; Burkhard, 1993; González-Casado and García-Cuevas, 1999) compare the strain tensors yielded by the strain gauge technique and other independent methods of stress/strain analysis and encountered similar results. The correlation between the principal strain/stress orientations established by twin analysis and by other methods is therefore fairly good. However, the strain values deduced from the strain gauge technique are difficult to correlate with the bulk strain because of the partitioning of the latter into different components (here, primarily into the grain-boundary sliding of the inoceramid shell prisms).

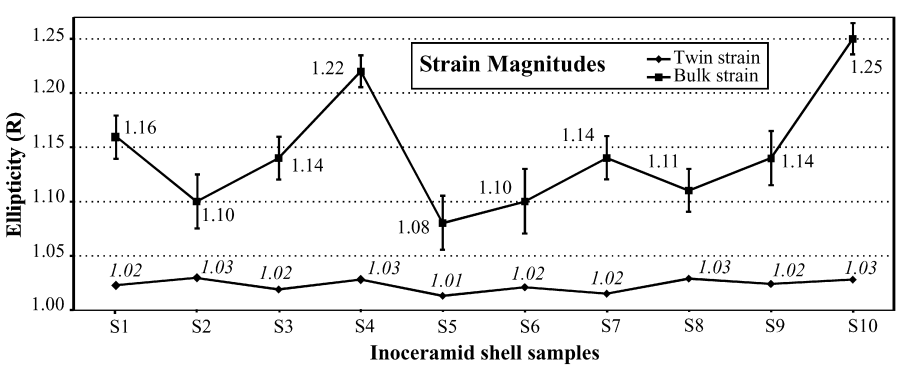

Fig. 4. Plot of twin strain versus bulk strain (ellipticity *R*) for the studied samples (S1–S10). Bars represent the calculated error for the centre to centre determinations.

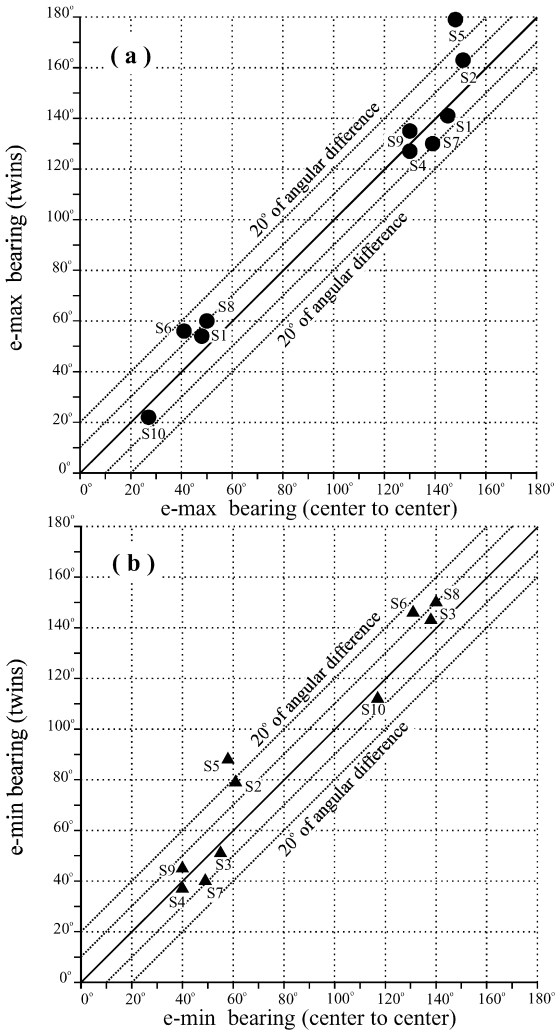

Fig. 5. Plot of the principal strains bearing deduced from the strain gauge technique and from the centre to centre method for each sample (S1–S10). Oblique lines represent angular differences between the principal extension bearings measured by both methods (differences of 0°, solid line; and differences of 10 and 20°, dashed lines). (a) Values for the e_{max} axis. (b) Values for the e_{min} axis.

5. Conclusions

The results presented here have been obtained from a new tectonic marker, inoceramid shells, which regularly built up an extraordinary aggregate of calcite pseudo-hexagonal prisms with a honeycomb microstructure. The inoceramid shell studied in this work underwent low-temperature deformation, resulting in the formation of a set of e-twins (a small fraction of the prisms shows two sets of twins) and other microstructures. The analysis of the low-temperature strain partitioning suggest that about 7–8 times the twin strain occurs by grain boundary sliding. In the context of a non-random distribution of calcite *c*-axes and 2D analysis, the strain gauge technique yields twin strain magnitudes that do not correlate with the finite strains determined by the Fry method. Under these conditions, results provided by the strain gauge technique must be interpreted with caution. However, the principal strain axis orientations calculated in the prisms by calcite e-twin analysis and by the centre to centre method agree adequately. Despite the uncertainties associated with the determination of the twin strain, the strain gauge technique appears to provide results that can be used to establish the principal strain orientations, even though the calcite prisms are crystallographically orientated. In conclusion, inoceramid shells can be successfully used as strain gauges to determine deformation in marine carbonate rocks.

Acknowledgements

This paper, part of a Ph.D. thesis by A. Jiménez-Berrocoso, was funded by UPV project 130.310-EB034/99 and MCyT project BTE2002-01742. We thank A. Burton for linguistic assistance. The manuscript was greatly improved by the comments of Prof. Groshong, two anonymous reviewers and the editor, Prof. Hippertt.

References

Burkhard, M., 1993. Calcite twins, their geometry, appearance and significance as stress-strain markers and indicators of tectonic regime: a review. Journal of Structural Geology 15, 351–368.

Craddock, J.P., Van der Pluijm, B.A., 1988. Kinematic analysis of an en échelon continuous vein complex. Journal of Structural Geology 10, 445–452.

Craddock, J.P., Nielson, K.J., Malone, D.H., 2000. Calcite twinning strain constraints on the emplacement rate and kinematic pattern of the upper plate of the Heart Mountain Detachment. Journal of Structural Geology 22, 983–991.

Cuevas, J., Eguiluz, L., Ramon-Lluch, R., Tubia, J.M., 1982. Sobre la existencia de una deformación tectónica compleja en el Flanco N del Sinclinal de Oiz-Punta Galea (Vizcaya): Nota preliminar, Lurralde. Investigación y Espacio 1, 47–62.

Elorza, J., García-Garmilla, F., 1996. Petrological and geochemical evidence for diagenesis of inoceramid bivalve shells in the Plentzia Formation (Upper Cretaceous, Basque–Cantabrian Region, northern Spain). Cretaceous Research 17, 479–503.

Evans, M.A., Dunne, W.M., 1991. Strain factorization and partitioning in the North Mountain thrust sheet, central Appalachians, USA. Journal of Structural Geology 13, 21–35.

Evans, M.A., Groshong Jr, R.H., 1994. A computer program for the calcite strain-gauge technique. Journal of Structural Geology 16, 277–281.

Ferrill, D.A., 1991. Calcite twin width and intensities as metamorphic indicators in natural low-temperature deformation of limestone. Journal of Structural Geology 13, 667–675.

Ferrill, D.A., Groshong Jr, R.H., 1993a. Determination conditions in the northern Subalpine Chain, France, estimated from deformations modes in coarse-grained limestones. Journal of Structural Geology 15, 995–1006.

Ferrill, D.A., Groshong Jr, R.H., 1993b. Kinematic model for the curvature of the northern Subalpine Chain, France. Journal of Structural Geology 15, 523–541.

Fry, N., 1979. Random point distributions and strain measurement in rocks. Tectonophysics 60, 89–105.

González-Casado, J.M., García-Cuevas, C., 1999. Calcite twins from microveins as indicators of deformation history. Journal of Structural Geology 21, 875–889.

González-Casado, J.M., García-Cuevas, C., 2002. Strain analysis from calcite e-twins in the Cameros basin, NW Iberian Chain, Spain. Journal of Structural Geology 24, 1777–1788.

Groshong, R.H. Jr, 1972. Strain calculated from twinning in calcite. Geological Society of America Bulletin 83, 2025–2048.

Groshong, R.H. Jr, 1974. Experimental test of the least-squares strain gauge calculation using twinned calcite. Geological Society of America Bulletin 85, 1855–1864.

Groshong, R.H. Jr, Pfiffner, O.A., Pringle, L.R., 1984a. Strain partitioning in the Helvetic thrust belt of eastern Switzerland from the leading edge to the internal zone. Journal of Structural Geology 6, 19–32.

Groshong, R.H. Jr, Teufel, L.W., Gasteiger, C., 1984b. Precision and accuracy of the calcite strain-gauge technique. Geological Society of America Bulletin 95, 357–363.

Harris, J.H., Van der Pluijm, B.A., 1998. Relative timing of calcite twinning strain and fold-thrust belt development; Hudson Valley fold-thrust belt, New York, USA. Journal of Structural Geology 20, 21–33.

Hindle, D.A., 1997. Quantify stresses and strains from the Jura Arc, and their usefulness in choosing and deformation model for the region. Ph.D. thesis, University of Neuchatel.

Jiménez-Berrocoso, A., Pascual, A., Elorza, J., 2001. Señales geoquímicas y micropaleontológicas como marcadores de eventos paleoceanográficos en el Santoniense del Arco Vasco. Geogaceta 30, 155–158.

Kilsdonk, B., Wiltschko, D.V., 1988. Deformation mechanisms in the southeastern ramp region of the Pine Mountain block, Tennessee. Geological Society of America Bulletin 100, 653–664.

López, G., Martínez, R., Lamolda, M.A., 1992. Biogeographic relationships of the Coniacian and Santonian inoceramid bivalves of northern Spain. Palaeogeography, Palaeoclimatology, Palaeoecology 92, 249–261.

MacLeod, K.G., 1994. Extinction of inoceramid bivalves in Maastrichtian strata of the Bay of Biscay region of France and Spain. Journal of Paleontology 68, 1048–1066.

MacLeod, K.G., Huber, B.T., Le Ducharme, M., 2000. Paleontological and geochemical constraints on the deep ocean during the Cretaceous greenhouse interval. In: Huber, B.T., MacLeod, K.G., Wing, S. (Eds.), Warm Climates in Earth History, Cambridge University Press, pp. 234–274.

Mathey, B., 1982. El Cretácico Superior del Arco Vasco, In: El Cretácico de España. Universidad Complutense de Madrid, pp. 111–136.

Mosar, J., 1989. Deformation interne dans les Préalpes Médianes (Suisse). Eclogae Geologicae Helvetiae 82, 765–794.

Pfiffner, O.A., Burkhard, M., 1987. Determination of paleostress axes orientations from fault, twin and earthquake data. Annales Tectonicae 1, 48–57.

Ramsay, J.G., Huber, M.I., 1983. The Techniques of Modern Structural Geology. Volume 1: Strain Analysis, Academic Press, London.

Saltzman, E.S., Barron, E.J., 1982. Deep circulation in the Late Cretaceous: oxygen isotope paleotemperatures from Inoceramus remains in D.S.D.P. cores. Palaeogeography, Palaeoclimatology, Palaeoecology 40, 167–181.

Weiss, L.E., 1954. A study of tectonic style: structural investigation of a marble quartzite complex in southern California. University of California Publications in Geological Science 30, 1–102.

Wiltschko, D.V., Medwedeff, D.A., Millson, H.E., 1985. Distribution and mechanisms of strain within rocks on the Northwest ramp of Pine Mountain block, southern Appalachian foreland: a field test of theory. Geological Society of America Bulletin 96, 426–435.